

Lattice dynamics of ferroelectric PbTiO₃ by inelastic neutron scattering

J. Hlinka,¹ M. Kempa,^{1,2,3} J. Kulda,³ P. Bourges,⁴ A. Kania,⁵ and J. Petzelt¹

¹*Institute of Physics, Academy of Sciences of the Czech Republic, Na Slovance 2, 18221 Praha 8, Czech Republic*

²*Faculty of Mathematics and Physics, Charles University, Ke Karlovu 5, 121 16 Praha 2, Czech Republic*

³*Institut Laue-Langevin, BP 156, 38042 Grenoble Cedex 9, France*

⁴*Laboratoire Léon Brillouin, C.E.A./C.N.R.S., F-91191 Gif-sur-Yvette CEDEX, France*

⁵*Institute of Physics, University of Silesia, ul. Uniwersytecka 4, 40007 Katowice, Poland*

(Received 7 January 2006; published 21 April 2006)

Room-temperature dispersion relations of the phonon modes associated with lead ion vibrations in ferroelectric PbTiO₃ single crystal have been investigated using inelastic neutron scattering. Both transverse acoustic and transverse optic modes propagating in the direction perpendicular to the spontaneous polarization show considerable splitting due to tetragonal anisotropy. The results of an earlier inelastic neutron scattering study are revised, and it is shown that the present picture is compatible with recent results obtained from Raman and Brillouin spectroscopy.

DOI: 10.1103/PhysRevB.73.140101

PACS number(s): 77.80.-e, 78.70.Nx, 63.20.Dj

PbTiO₃, a prototype¹ ferroelectric perovskite crystal with a Pm $\bar{3}$ m parent high-temperature phase, is a popular model system for various phenomenological¹⁻⁵ and first-principles-based⁶⁻¹⁹ calculations. It has a fairly high Curie temperature¹ ($T_C=760$ K) and a large spontaneous strain¹ (at ambient conditions, $c/a=1.06$). The transition to its tetragonal ferroelectric phase ($\mathbf{P}_S\parallel c$) is of an essentially displacive type, associated with a well-defined zone-center soft mode, whose frequency drops down to about²⁰ 50 cm^{-1} . In contrast to many other ABO₃ perovskites with a ferroelectric soft mode, such as BaTiO₃, SrTiO₃, or KNbO₃, the eigenvector of the PbTiO₃ soft mode corresponds primarily to A atoms vibrating against the BO₆ octahedra, i.e., to the so-called Last mode.²¹ The ferroelectric phase transition can be also attained at room temperature by applying hydrostatic pressure ($p_C=12$ GPa), but the exact pressure phase diagram is still under debate.^{22,23} In materials science, lead titanate is frequently used to dilute other complex lead-based perovskites, such as Pb(Mg_{1/3}Nb_{2/3})O₃, Pb(Zn_{1/3}Nb_{2/3})O₃, or (Pb,La)ZrO₃ to increase their piezoelectric properties by increasing their phase transition temperature or by bringing them closer to the so-called morphotropic phase boundary.^{24,25}

Lattice vibration spectra of PbTiO₃ have been subject to numerous detailed studies, mainly by Raman spectroscopy (e.g., Refs. 20, 22, and 26–30) as well as by *ab initio* calculations (e.g., Refs. 22 and 31–34). Experimentally, only little is known about the dispersion of its phonon branches, even though this is quite important for example in the context of the long-standing controversy about the origin of diffuse scattering in perovskite ferroelectrics (see Ref. 35 and references therein). Indeed, the only available results were reported in the pioneering inelastic neutron scattering study of Shirane *et al.*,³⁶ which describes dispersion of the soft mode and of some acoustic branches in both cubic and ferroelectric phases. However, the picture is incomplete: For example, it follows from symmetry considerations that the soft mode branch propagating in the direction perpendicular to the spontaneous polarization should be split into a pair of

$\Delta_1-\Delta_2$ branches (associated with E_{TO} and A_{1TO} zone center modes). Moreover, Raman scattering experiments imply that at room temperature there should be an additional branch lying just in between them (associated with the lowest-frequency E_{LO} zone center mode). The purpose of this study is to investigate these missing branches in order to complete the chart of the low-frequency phonon dispersion curves in ferroelectric PbTiO₃.

Our experiment was carried out on the 1 T thermal neutron three-axis spectrometer at the ORPHEE reactor of the Laboratoire Leon Brillouin, CEA-Saclay. The instrument was operated in its standard configuration, using horizontally and vertically focusing monochromator and analyzer crystals (PG 002) together with a natural collimation. All of our measurements were performed at a fixed energy of scattered neutrons (14.7 meV) with a pyrolytic graphite filter in front of the analyzer. A typical full width at half maximum (FWHM) energy resolution of 0.95 meV was verified by measuring the incoherent elastic scattering of the sample.

The sample used in this study was a high-quality 2.7 mm thick single-crystal platelet (700 mg) with optically perfect natural faces, selected from a series of crystals grown by the flux method. The PbO-B₂O₃ system was used as a solvent and the crystallization was carried out in the temperature range of 1050–900 °C with a cooling rate of 0.7 °C/h; more details are given in Ref. 37. No ferroelastic domain walls were seen under the polarized light microscope and neutron diffraction has confirmed that the tetragonal axis (c) was perpendicular to the platelet in at least 95% of the sample volume. The sample was mounted with its c axis ($[001]$) either horizontal or vertical, in order to access the transverse modes polarized parallel as well as perpendicular to the spontaneous polarization direction.

To obtain the phonon frequencies shown in Fig. 1, the neutron spectra were fitted with a superposition of a model of independent damped harmonic oscillators together with a slowly varying background, convoluted with a four-dimensional Gaussian instrumental resolution function $R(\mathbf{Q}, \omega)$, assuming a locally linearized dispersion relation

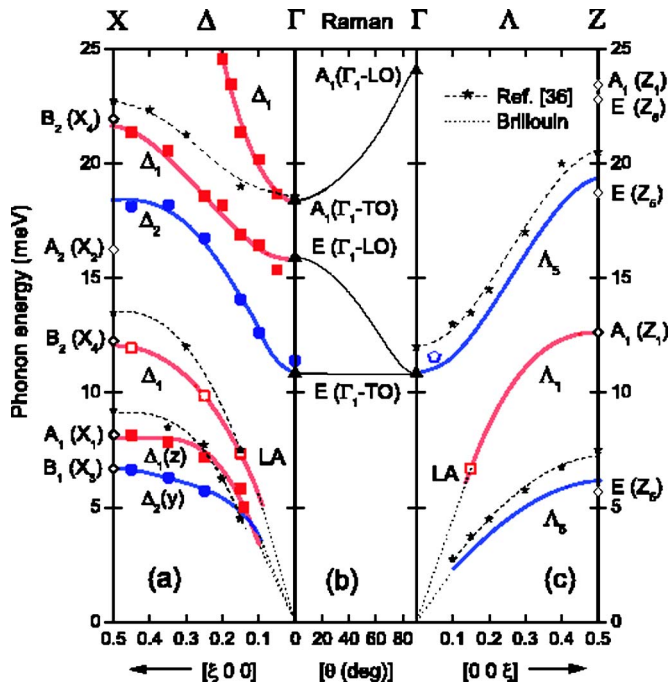


FIG. 1. (Color online) Low-frequency phonon dispersion curves of PbTiO_3 at ambient temperature. (a) Dispersion relation along the $[100]$ direction. (b) Angular dispersion of long-wavelength modes with wave vectors rotating from $[100]$ to $[001]$ direction. (c) Dispersion relation along $[001]$ direction. Larger symbols stand for the data from this study (open squares— Δ_1 and Λ_1 longitudinal acoustic branches, solid squares— Δ_1 transverse acoustic (TA) branches, solid circles— Δ_2 branches, open pentagon: Λ_5 mode shown in Fig. 3), smaller symbols are from literature (solid triangles—Raman experiment of Ref. 28, stars—inelastic neutron scattering of Ref. 36, open diamonds—*ab initio* results of Ref. 34). Dotted lines stand for linear acoustic dispersion extrapolated from Brillouin data of Refs. 43 and 44, dashed and solid lines are guides for the eyes.

and using the program packages AFITV (Ref. 38) and/or RESTRAX.³⁹ Both fitting programs converged to the same phonon frequencies. A relatively high but smooth and monotonic inelastic background, which can be partly due to the scattering by air and/or tiny traces of the plastic glue on one of the edges of the crystal, was held almost constant for all spectra.

Our investigation was mostly focused on the low-frequency modes propagating along the $[100]$ direction [see Fig. 1(a)]. The little group of $(\xi 0 0)$ wave vectors is m_y , and there are thus only two symmetry species having eigenvectors symmetric (Δ_1) or antisymmetric (Δ_2) with respect to the m_y plane (symmetry analysis of phonon vibrations of ferroelectric PbTiO_3 can be found, e.g., in Refs. 34 and 40; labeling of experimental dispersion is done with the usual Bouckaert-Smoluchowski-Wigner⁴¹ notation as described in Ref. 42, the correspondence⁴² with Mulliken notation system is given in Fig. 1). Mode assignments are based on the fact that the inelastic structure factor scales with a scalar product of the phonon eigenvector and the momentum transfer \mathbf{Q} . For example, the representative neutron spectra corresponding to the transverse optic (TO) modes displayed in Fig. 2 were taken at momentum transfers of $(0.15 0 2)$ and

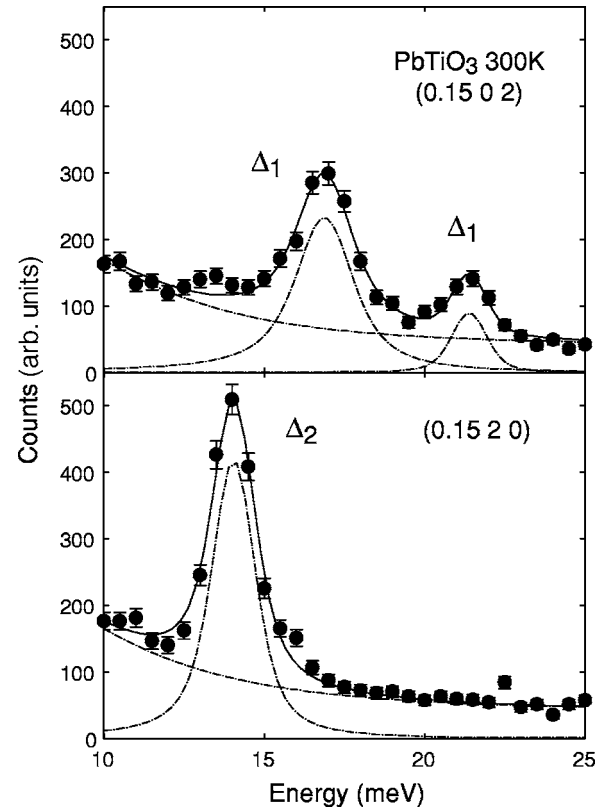


FIG. 2. Inelastic neutron scattering spectra from constant- \mathbf{Q} scans with momentum transfers of $(0.15 0 2)$ and $(0.15 2 0)$, revealing the Δ_1 (top) and Δ_2 (bottom) transverse optic modes. Point symbols stand for the data points, the solid line corresponds to the fit with the damped harmonic oscillator model, the dashed lines represent the individual components of the model.

$(0.15 2 0)$ so that the corresponding mode eigenvectors are expected to have significant projections onto the $[001]$ and $[010]$ directions, respectively. Consequently, they can be assigned to Δ_1 and Δ_2 species, respectively.

Close to the Brillouin zone center, all three observed optic branches [see Fig. 1(a)] approach the frequencies of E_{TO} , E_{LO} , and $A_{1\text{TO}}$ modes known from Raman experiments.²⁸ It is worth noting that interpretation of direct measurements of the Brillouin zone center modes by the inelastic neutron scattering technique is problematic in the present case, because of the angular dispersion of the oblique long-wavelength soft optic modes as a function of the angle θ between the phonon wave vector and the xy plane. This angular dispersion calculated according to Raman spectroscopy data as in Ref. 28 is shown in Fig. 1(b).

Similarly, the course of the acoustic branches fits well with the limiting slopes of long-wavelength acoustic phonon modes determined from Brillouin experiments^{43,44} [see Fig. 1(a)]. Here, it is interesting to note that the observed y -polarized (Δ_2) TA modes have significantly lower frequencies than the z -polarized (Δ_1) TA modes, even though Brillouin scattering results^{43,44} show that at long wavelengths the situation is just the opposite ($C_{66} > C_{44}^D$). This implies an upward bending of the (Δ_1) TA branch and crossing of the two TA modes at some finite wave vector. Such upward bending

of the (Δ_1) TA branch was already observed⁴⁵ in tetragonal BaTiO_3 .

The acoustic branches are expected to be dominated by vibrations of the heavy lead atoms,³² which suggests³⁴ the assignment of the associated X-point zone boundary modes of y , z , and x polarized acoustic branches as $B_1(X_3)$, $A_1(X_1)$, and $B_2(X_4)$ modes. These, as well as the higher-frequency X-point modes can be also assigned from their correspondence with the *ab initio* predicted frequencies.³⁴ As a matter of fact, there is a remarkable agreement between the calculations³⁴ and experiment (see Fig. 1), probably due to the fact that the anharmonic effects are quite small at room temperature in this crystal.

Comparing our results with the data obtained in the previous inelastic neutron scattering results³⁶ displayed in Fig. 1, we have to bear in mind that probably, contrary to the present work, no measurement was done for sample orientation with the c axis vertical. Consequently, the transverse Δ_2 species were not observable in the previous study (see Fig. 2). The absence of the second optic branch in the previous results is more puzzling. But it is possible that the dynamic structure factor of the missing modes was too small in the Brillouin zone used for their measurements. At the same time, it appears that all of the previously measured frequencies are systematically by about 10–15% higher than the present ones. As we are not aware of any calibration problem in the present experiment and as our observed frequencies are supported by the optical spectroscopy results, we believe that the discrepancy is due either to instrumental problem in the previous experiment or, more probably, inherent in the sample used in the previous experiment. In fact, it is reported³⁶ that the sample was a “composite” assembly of five crystals (with a possible residual ferroelastic twinning), and moreover, the sample was slightly doped by uranium atoms, which might have created a lattice strain, leading to a phonon frequency upshift.

For the modes propagating along the tetragonal axis, whose dispersion is indicated in Fig. 1(c), the two-fold degeneracy of transverse branches is preserved (Λ modes are classified according to 4 mm point group). Therefore, the dispersion scheme of Λ_5 branches as given in Ref. 36 is correct, and no other branches are expected below 20 meV except for the LA Λ_1 branch. Dispersion of the latter can be well guessed by interpolating between the low- q slope from Brillouin experiments^{43,44} and the *ab initio* predicted³⁴ frequency of the associated zone boundary mode [we have determined one additional point, see Fig. 1(c)]. Most likely, the Λ_5 phonon frequencies of Ref. 36 are also overestimated by 10–15%. For example, the measurement of the Λ_5 TO mode at $\mathbf{Q}=(20-0.05)$ shown in Fig. 3, gives a phonon frequency much closer to the Raman value²⁸ of the E_{TO} mode than to the previous inelastic neutron scattering³⁶ result. The tentative renormalization by 15% of the Λ_5 phonon data of Ref. 36 is therefore indicated by solid lines drawn in Fig. 1(c).

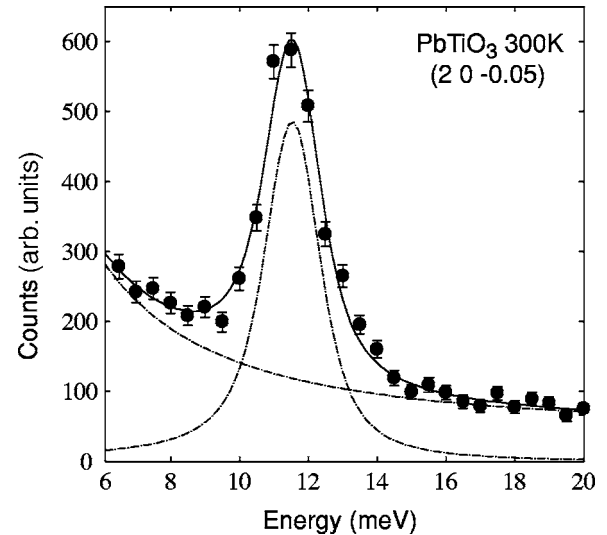


FIG. 3. Inelastic neutron scattering spectrum of long-wavelength Λ_5 TO phonon taken at $\mathbf{Q}=(20-0.05)$. Point and line symbols have the same meaning as in Fig. 2.

It is instructive to consider the observed transverse phonon branches as derived from the double degenerate Δ_5 branches of the parent cubic phase. In the ferroelectric phase, the Δ_5 TA modes propagating along the $[001]$ axis are merely “renamed” as Λ_5 modes, while those propagating along the $[100]$ axis split in a Δ_1 - Δ_2 pair. The same holds for the Δ_5 TO branch, except that the presumably rather flat transverse Δ_1 component interacts with another very steep soft longitudinal Δ_1 branch associated with the E_{LO} zone center mode. The strong eigenvector exchange between the two Δ_1 branches could be the reason why their anticrossing was missed earlier. It is also interesting to note that for both the TA and TO modes, the y -polarized Δ_2 split components have lower frequencies than their z -polarized Δ_1 partners.

In conclusion, our present neutron data for long-wavelength phonon modes are perfectly consistent with the results of recent Raman and Brillouin scattering studies. Also, they are in good agreement with the frequencies of zone boundary modes predicted by *ab initio* calculations. On top of that, our results reveal a remarkable tetragonal anisotropy in the ferroelectric phase of PbTiO_3 . This more complete picture of low-energy phonon dispersion curves in PbTiO_3 will provide a reference for comparison with other perovskites, such as lead-based relaxor ferroelectrics, exhibiting Last-type soft modes.

This project has been supported by the Grant Agency of the Czech Republic (Project Nos. 202/06/0411 and 202/04/0993). The experiment at LLB was supported by the European Commission under the 6th Framework Programme through the Key Action: Strengthening the European Research Area, Research Infrastructures, Contract No. RII3-CT-2003-505925 (NMI3).

- ¹M. E. Lines and A. M. Glass, *Principles and Applications of Ferroelectrics and Related Materials* (Oxford University Press, Oxford, 2001).
- ²V. G. Koukhar, N. A. Pertsev, and R. Waser, *Phys. Rev. B* **64**, 214103 (2001).
- ³M. Budimir, D. Damjanovic, and N. Setter, *Phys. Rev. B* **72**, 064107 (2005).
- ⁴S. C. Costa, P. S. Pizani, J. P. Rino, and D. S. Borges, *J. Phys.: Condens. Matter* **17**, 5771 (2005).
- ⁵R. Ramirez, M. F. Lapena, and J. A. Gonzalo, *Phys. Rev. B* **42**, 2604 (1990).
- ⁶M. Dawber, K. M. Rabe, and J. F. Scott, *Rev. Mod. Phys.* **77**, 1083 (2005).
- ⁷O. Dieguez, K. M. Rabe, and D. Vanderbilt, *Phys. Rev. B* **72**, 144101 (2005).
- ⁸M. Ghita, M. Fornari, D. J. Singh, and S. V. Halilov, *Phys. Rev. B* **72**, 054114 (2005).
- ⁹C. Lichtensteiger, J.-M. Triscone, J. Junquera, and P. Ghosez, *Phys. Rev. Lett.* **94**, 047603 (2005).
- ¹⁰H. Mestric, R.-A. Eichel, T. Kloss, K.-P. Dinse, S. Laubach, St. Laubach, P. C. Schmidt, K. A. Schonau, M. Knapp, and H. Ehrenberg, *Phys. Rev. B* **71**, 134109 (2005).
- ¹¹M. Sepliarsky, M. G. Stachiotti, and R. L. Migoni, *Phys. Rev. B* **72**, 014110 (2005).
- ¹²M. Veithen, X. Gonze, and Ph. Ghosez, *Phys. Rev. Lett.* **93**, 187401 (2004).
- ¹³S. Tinte, K. M. Rabe, and D. Vanderbilt, *Phys. Rev. B* **68**, 144105 (2003).
- ¹⁴H. Fu and L. Bellaiche, *Phys. Rev. Lett.* **91**, 057601 (2003).
- ¹⁵L. He and D. Vanderbilt, *Phys. Rev. B* **68**, 134103 (2003).
- ¹⁶B. Meyer and D. Vanderbilt, *Phys. Rev. B* **65**, 104111 (2002).
- ¹⁷C. H. Park and D. J. Chadi, *Phys. Rev. Lett.* **84**, 4717 (2000).
- ¹⁸G. Saghi-Szabo, R. E. Cohen, and H. Krakauer, *Phys. Rev. Lett.* **80**, 4321 (1998).
- ¹⁹R. E. Cohen, *Nature (London)* **358**, 136 (1992).
- ²⁰G. Burns and B. A. Scott, *Phys. Rev. Lett.* **25**, 167 (1970).
- ²¹J. T. Last, *Phys. Rev.* **105**, 1740 (1957).
- ²²I. A. Kornev, L. Bellaiche, P. Bouvier, P. E. Janolin, B. Dkhil, and J. Kreisel, *Phys. Rev. Lett.* **95**, 196804 (2005).
- ²³Z. Wu and R. E. Cohen, *Phys. Rev. Lett.* **95**, 037601 (2005).
- ²⁴B. Noheda, D. E. Cox, G. Shirane, S. E. Park, L. E. Cross, and Z. Zhong, *Phys. Rev. Lett.* **86**, 3891 (2001).
- ²⁵S. E. Park and T. R. Shrout, *J. Appl. Phys.* **82**, 1804 (1997).
- ²⁶J. A. Sanjurjo, E. Lopez-Cruz, and G. Burns, *Phys. Rev. B* **28**, 7260 (1983).
- ²⁷M. D. Fontana, H. Idrissi, C. E. Kugel, and K. Wojcik, *J. Phys.: Condens. Matter* **3**, 8695 (1991).
- ²⁸C. M. Foster, Z. Li, M. Grimsditch, S. K. Chan, and D. J. Lam, *Phys. Rev. B* **48**, 10160 (1993).
- ²⁹S. M. Cho and H. M. Jang, *Appl. Phys. Lett.* **76**, 3014 (2000).
- ³⁰D. Fu, H. Suzuki, and K. Ishikawa, *Phys. Rev. B* **62**, 3125 (2000).
- ³¹W. Zhong, R. D. King-Smith, and D. Vanderbilt, *Phys. Rev. Lett.* **72**, 3618 (1994).
- ³²P. Ghosez, E. Cockayne, U. V. Waghmare, and K. M. Rabe, *Phys. Rev. B* **60**, 836 (1999).
- ³³U. V. Waghmare and K. M. Rabe, *Phys. Rev. B* **55**, 6161 (1997).
- ³⁴A. García and D. Vanderbilt, *Phys. Rev. B* **54**, 3817 (1997).
- ³⁵B. D. Chapman, E. A. Stern, S. W. Han, J. O. Cross, G. T. Seidler, V. Gavril'yatchenko, R. V. Vedrinskii, and V. L. Kraizman, *Phys. Rev. B* **71**, 020102(R) (2005).
- ³⁶G. Shirane, J. D. Axe, J. Harada, and J. P. Remeika, *Phys. Rev. B* **2**, 155 (1970).
- ³⁷A. Kania, A. Slodczyk, and Z. Ujma, *J. Cryst. Growth* **289**, 134 (2006).
- ³⁸B. Hennion and P. Bourges, AFITV: Refinement program for triple axis spectrometer data at Laboratoire Leon Brillouin CEA/Saclay, France.
- ³⁹J. Kulda and J. Saroun, *Nucl. Instrum. Methods Phys. Res. A* **379**, 155 (1996).
- ⁴⁰J. D. Freire and R. S. Katiyar, *Phys. Rev. B* **37**, 2074 (1988).
- ⁴¹L. P. Bouckaert, R. Smoluchowski, and E. Wigner, *Phys. Rev.* **50**, 58 (1936).
- ⁴²L. S. Altmann and A. P. Cracknell, *Rev. Mod. Phys.* **37**, 19 (1965).
- ⁴³Z. Li, M. Grimsditch, C. M. Foster, and S. K. Chan, *J. Phys. Chem. Solids* **57**, 1433 (1996).
- ⁴⁴A. G. Kalinichev, J. D. Bass, B. N. Sun, and D. A. Payne, *J. Mater. Res.* **12**, 2623 (1997).
- ⁴⁵G. Shirane, J. D. Axe, J. Harada, and A. Linz, *Phys. Rev. B* **2**, 3651 (1970).